

Article

Time-Series Analysis of Isotope Composition of Precipitation in Zagreb, Croatia

Damir Borković ¹, Zoran Kovač ² and Ines Krajcar Bronić ^{1,*}

¹ Laboratory for Low-Level Radioactivities, Division of Experimental Physics, Ruder Bošković Institute, 10000 Zagreb, Croatia; damir.borkovic@irb.hr

² Faculty of Mining, Geology and Petroleum Engineering, University of Zagreb, 10000 Zagreb, Croatia; zoran.kovac@rgn.hr

* Correspondence: krajcar@irb.hr

Abstract: Air temperature and precipitation data (1976–2021), stable isotope composition ($\delta^{18}\text{O}$, $\delta^2\text{H}$) data, and deuterium excess (1980–2021) data were analyzed using principal component analysis (PCA), Fourier analysis (FA), and wavelet analysis (WA). The PCA represented each month by a single dot in the diagram, and month 1 and month 7 were clearly distinguished. The FA and WA gave the 12-month period for all parameters, but the strongest power was for temperature, then $\delta^{18}\text{O}$ and $\delta^2\text{H}$, and finally for the precipitation amount and deuterium excess. Both Pearson's r and Spearman's ρ correlation coefficients gave similar values for $\delta^2\text{H}$ — $\delta^{18}\text{O}$ and temperature— $\delta^2\text{H}$, $\delta^{18}\text{O}$ correlations.

Keywords: principal component analysis (PCA); Fourier analysis (FA); wavelet analysis (WA); precipitation



Citation: Borković, D.; Kovač, Z.; Krajcar Bronić, I. Time-Series Analysis of Isotope Composition of Precipitation in Zagreb, Croatia. *Water* **2022**, *14*, 2008. <https://doi.org/10.3390/w14132008>

Academic Editor: Maurizio Barbieri

Received: 23 May 2022

Accepted: 21 June 2022

Published: 23 June 2022

Publisher's Note: MDPI stays neutral with regard to jurisdictional claims in published maps and institutional affiliations.



Copyright: © 2022 by the authors. Licensee MDPI, Basel, Switzerland. This article is an open access article distributed under the terms and conditions of the Creative Commons Attribution (CC BY) license (<https://creativecommons.org/licenses/by/4.0/>).

1. Introduction

A statistical technique that deals with time-series data is called a time-series analysis. Time-series data mean that the data are in a series of particular time periods or any other intervals. It is used by many industries in order to extract meaningful statistics, characteristics, and insights. Among time-series analysis, Fourier analysis (FA) and wavelet analysis (WA) have proven to be powerful tools for detecting temporal variations in time-series data.

Principal component analysis (PCA) is a dimensionality-reducing method that is used to reduce the dimensionality of large data sets by transforming a large set of variables into a smaller one that still contains most of the information in the large set. Such a small dimensionality set can be easily visualized and analyzed.

The strength of the relationship between the two variables is called a correlation coefficient, and its values range between -1.0 and 1.0 . A correlation of -1.0 is a perfect negative correlation, while a correlation of 1.0 is a perfect positive correlation. A correlation of 0.0 shows no linear relationship between the two variables.

Few stations have enough data to perform wavelet data analysis. About one-sixth of the number of complete cycles can be confidently found [1]. Therefore, at least 6 years of the data record is needed for accurate and precise determination of 1-year seasonal fluctuations. The longer the observation time, the higher the accuracy and precision in evidencing the cycles and their time span.

Most of the WA were used to study global long-term periods [2–7]. Some were used to teleconnect large-scale climate indices and hydrochemical and isotopic characteristics of a karst spring [8] or to study spatio-temporal variability of rainfall and streamflows over the last decades [9].

Only a few studies have been applied to tritium analyses [10,11] or stable isotopes in precipitation [12]. Wavelet analysis was used to determine tritium variation in precipitation for several stations with long-term data and correlate them with solar activity fluctuations [10] and determine solar cycle periodicity in tritium activity in precipitation in Zagreb from 1996 to 2019 [11]. Time-series analysis (both FA and WA) was applied to a 7-year

record (2012–2018) of $\delta^{18}\text{O}$, $\delta^2\text{H}$, deuterium excess in precipitation, as well as temperature and precipitation amount [12].

The history of monitoring isotope data in precipitation at Zagreb is much longer than the minimum of seven years—tritium has been monitored since 1976, while stable isotope data are available for 1980–2006 and from 2012 onward. The series of data is rather scarce in Europe [13], and it deserves to be analyzed in many different ways. Statistical analysis of ^3H activity concentration, $\delta^2\text{H}$, $\delta^{18}\text{O}$, and deuterium excess and comparison with basic meteorological data (temperature, amount of precipitation) was presented in [14], but no principal component analysis was performed, and no Fourier and wavelet analysis was performed. Mean annual temperature showed a statistically significant increase of $0.07\text{ }^\circ\text{C}$ per year. Annual mean $\delta^{18}\text{O}$ and $\delta^2\text{H}$ values showed an increase of 0.017‰ and 0.14‰ per year, respectively, resembling an increase in the temperature. The mean yearly precipitation amount did not show any statistically significant change, but the annual values showed higher dispersion from the mean during the last 20 years. The distribution of the monthly amount of precipitation moved to the second half of the year, with the maximum in September. The mean deuterium excess remained constant over the years, but a change of distribution was observed: a decrease in deuterium excess in the first half of the year and an increase in the second half (maximum in November) due to air masses coming from the eastern Mediterranean.

Long-term (1980–2021) isotope data ($\delta^2\text{H}$, $\delta^{18}\text{O}$, deuterium excess) of monthly precipitation in Zagreb were studied here using statistical time-series analyses. Data for meteorological parameters for 1976–2021 (mean monthly air temperature and the monthly amount of precipitation) were also included. We used the data presented in [14] complemented with the new data from 2019–2021 (Supplementary File, Table S1). Principal component analysis, Fourier analysis, and wavelet analysis were used to determine what kind of results could be obtained. The principal question was whether this kind of analysis could show any dependence on temperature. Finally, we compared the two correlation coefficients (Pearson's r and Spearman's ρ) to determine any possible difference between them.

2. Materials and Methods

Two frequency analysis methods were used: periodogram (Fourier analysis) and wavelet. The algorithm for both methods used supports evaluating unevenly spaced data points.

Unevenly and missing spaced data points could be converted to evenly spaced points in a few different ways, such as interpolation, setting missing data points to zeros, and others. However, practice showed that these methods are not reassuring. Therefore, for periodogram analysis, we chose the Lomb periodogram [15]. In our case, N data points ($h_i \equiv h(t_i)$, $i = 1, \dots, N$) are measured at unevenly sampled times t_i . The Lomb normalized periodogram is given by

$$P_N(\omega) = \frac{1}{2\sigma^2} \left\{ \frac{[\sum_j (h_j - \bar{h}) \cos \omega(t_j - \tau)]^2}{\sum_j \cos^2 \omega(t_j - \tau)} + \frac{[\sum_j (h_j - \bar{h}) \sin \omega(t_j - \tau)]^2}{\sum_j \sin^2 \omega(t_j - \tau)} \right\} \quad (1)$$

where τ , \bar{h} , and σ^2 are defined by

$$\tan(2\omega\tau) = \frac{\sum_j \sin 2\omega t_j}{\cos 2\omega t_j} \quad (2)$$

$$\bar{h} = \frac{1}{N} \sum_1^N h_i \quad (3)$$

$$\sigma^2 = \frac{1}{N-1} \sum_1^N (h_i - \bar{h})^2 \quad (4)$$

and angular frequency $\omega = 2\pi f$, f being the frequency. The significance level of any peak in $P_N(\omega)$ is given by $1 - (1 - e^{-P_N(\omega_0)})^M$ for some concrete ω_0 , and M stands for the number of independent frequencies. The method used for fast calculation of $P_N(\omega)$ and M can be found in [16].

To analyze signal transient and/or non-sinusoidal nature, wavelet analysis was chosen. The algorithm for unevenly spaced data proposed by [17] was used. For the mother wavelet, Morlet wavelet $f(z) = e^{-cz^2}(e^{iz} - e^{-1/4c})$ with $c = 1/72$ was used [1].

Our data can be viewed as a multidimensional point consisting of five variable vectors $(x_1, x_2, x_3, x_4, x_5)$, where each point corresponds to a particular month of the year. The vector components x_i corresponds to temperature, $\delta^{18}\text{O}$, $\delta^2\text{H}$, precipitation, and deuterium excess. Such arranged data are suitable for principal component analysis (PCA) [18] in the points where all variables are present—in our case, 416 data points in total. Two principal components (PC1 and PC2) were used to present the data point, and the confidence ellipse and centroid were calculated. The confidence ellipses were calculated assuming bivariate Gaussian distribution. The centroid point (X, Y) for k points (x_i, y_i) , $i = 1, \dots, k$, was derived as follows:

$$X = \frac{1}{k} \sum_{i=1}^k x_i \quad (5)$$

$$Y = \frac{1}{k} \sum_{i=1}^k y_i \quad (6)$$

Both Pearson's and Spearman's methods were used to measure the correlation between the data. Pearson's correlation coefficient r evaluates the linear relationship between two continuous variables, while the Spearman correlation coefficient ρ is based on the ranked values for each variable rather than on the raw data. Both the correlation coefficients give a positive (or negative) correlation value, but the values can be different because Pearson's r measures δ , the linear relationship between the variables, while Spearman's ρ only measures monotonic relationships.

New stable isotope data ($\delta^2\text{H}$ and $\delta^{18}\text{O}$ of Zagreb's precipitation), related to the period 2019–2021, were determined at the Laboratory for Spectroscopy of the Faculty of Mining, Geology, and Petroleum Engineering, University of Zagreb, with a Liquid Water Isotope Analyzer (LWIA-45-EP, Los Gatos Research, San Jose, CA, USA). Data were analyzed by the Laboratory Information Management System (LIMS) [19]. The measurement precision of duplicates was $\pm 0.19\%$ for $\delta^{18}\text{O}$ and $\pm 0.9\%$ for $\delta^2\text{H}$.

3. Results

The temperature in 2019–2021 showed an increase in the lowest temperature and steady highest temperature in the last 5 years [13], which gave 2019 the title of the hottest year of the whole period of 1976–2021. Similar conclusions are also valid for $\delta^{18}\text{O}$ and $\delta^2\text{H}$ data. The annual mean deuterium excess is constant throughout 1980–2018, but with higher values in autumn than in spring, and this difference increased over time [14]. Deuterium excess for 2019–2021 was around 8‰ for January–August, while for September–December, it was higher than in all other periods, including 2012–2018 [14], reaching the average value of 14‰ in November. The average amount of precipitation did not change in 1976–2018, but larger fluctuations around the mean values were observed during the most recent period [14]. Precipitation in 2019–2021 was average (± 1 standard deviation), equal to the average value of 1976–2018.

3.1. PCA Analysis

PCA analysis (Figure 1) shows data points for months 1 and 7, together with their confidence ellipses. Those two months, each representing a different season, can be statistically separated in the PC1-PC2 space. The PC1 axis accounts for 56.27% of the variability, and PC2 for 25.04% of the variability in the data. We can also see that temperature, $\delta^{18}\text{O}$, and $\delta^2\text{H}$ are more closely aligned with the PC1 axis, and precipitation and deuterium

excess are linked with the PC2 axis. This leads to the conclusion that the winter/summer difference is most pronounced in temperature, $\delta^{18}\text{O}$, and $\delta^2\text{H}$ changes.

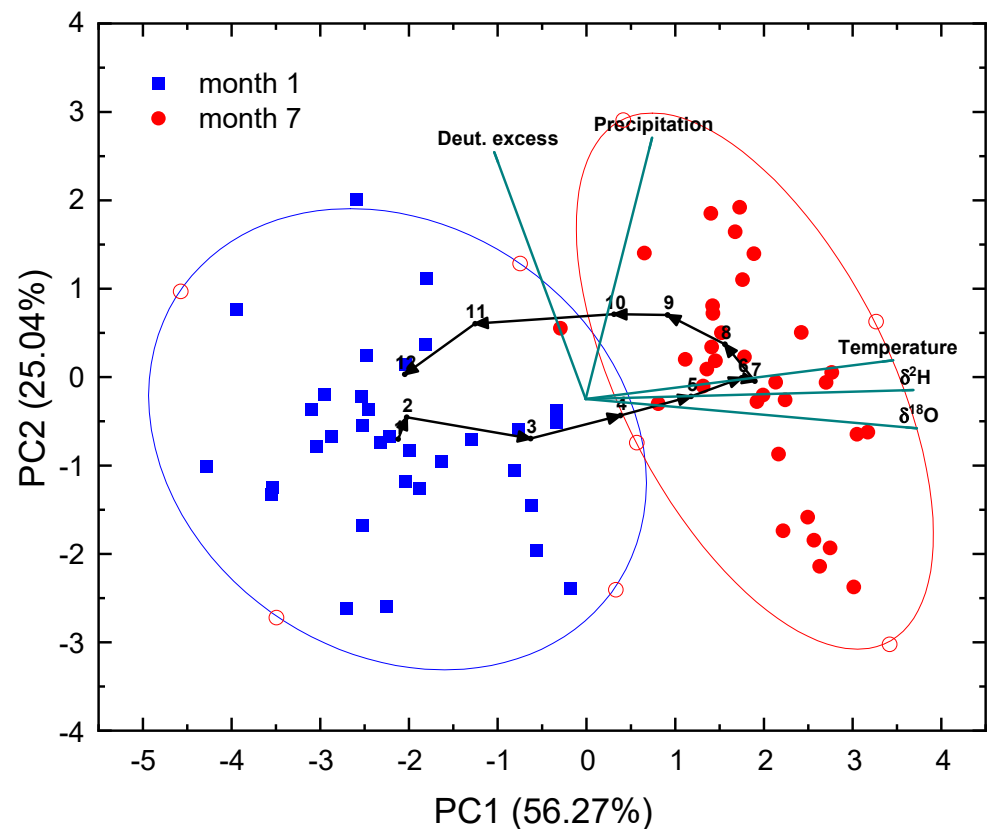


Figure 1. PCA of month 1 (blue squares) and month 7 (red dots); black dots connected with arrows represent each month in the year.

Additionally, Figure 1 shows centroids from all twelve months, with their path in the PC1-PC2 space denoted here by vectors marked with the numbers of the month. Such a representation further emphasizes that warmer months are mostly on the right side of the PC1 axis, corresponding to a higher temperature, $\delta^{18}\text{O}$, and $\delta^2\text{H}$. On the PC2 axis, precipitation and deuterium excess dominate. Months 3, 4, and 5 are separated from 11, 10, and 9, suggesting that the latter have more precipitation and a greater excess of deuterium. Here, the difference is less pronounced than on the PC1 axis.

3.2. FA Analysis

Fourier analysis (FA) of the temperature, $\delta^{18}\text{O}$, and $\delta^2\text{H}$ values (Figure 2a,b and S1) showed the strongest peaks. All peaks were well above the significance level of $p = 0.05$. The peak appeared at 12.01 months since those values exhibit strong annual seasonality. However, the increase in temperature due to global climate changes in recent decades cannot be seen [14].

FA of the precipitation amount (Figure 2c) and deuterium excess (Figure 2d) showed more frequencies, although the mean frequency is still one year, and others are not statistically significant. The 1-year peak is still well above the limit of $p = 0.05$, but the power of the peak (~30) is significantly lower than that of temperature (~250) or $\delta^{18}\text{O}$ and $\delta^2\text{H}$ (~120).

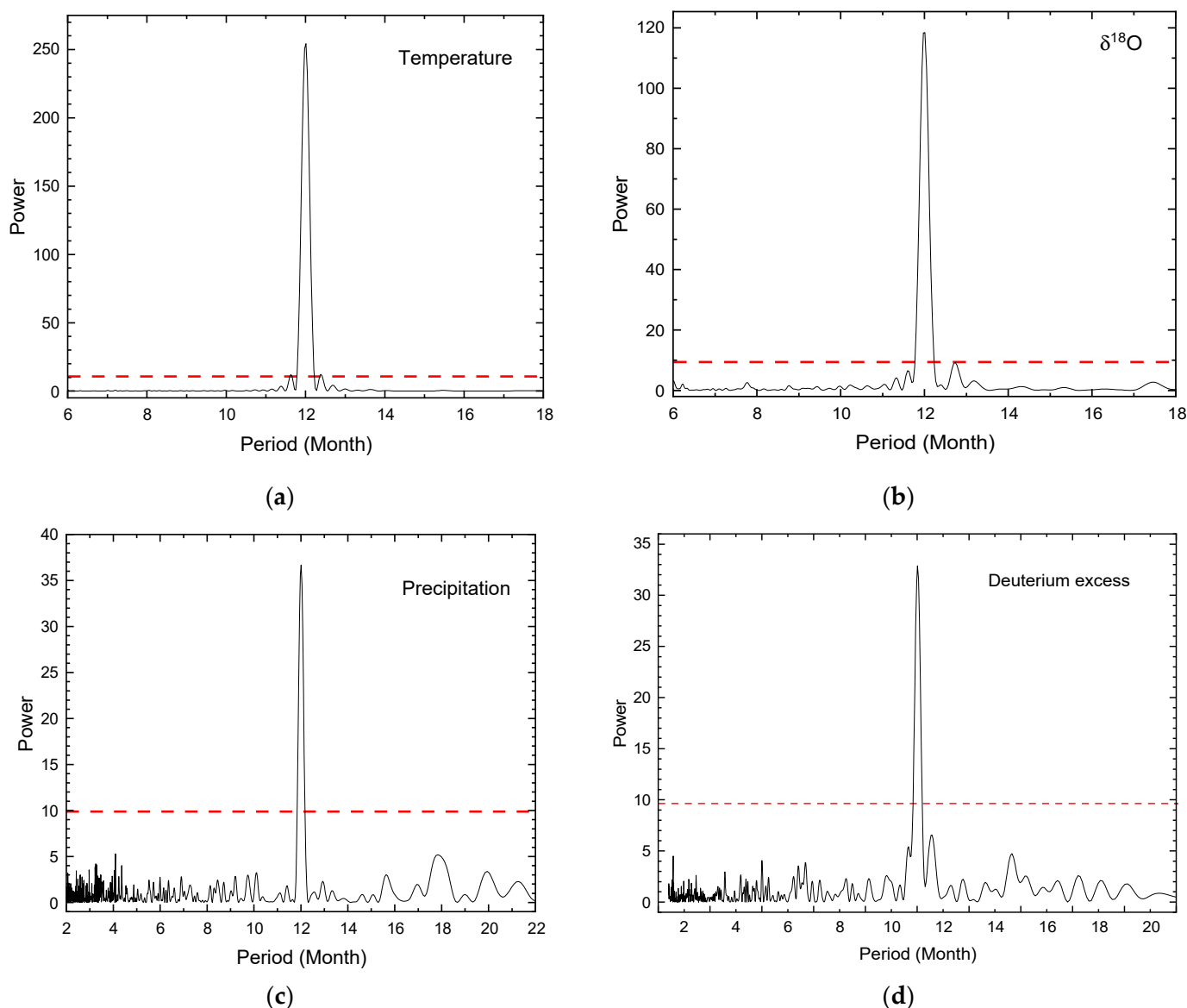


Figure 2. Fourier analysis (FA) graphs of: (a) temperature; (b) $\delta^{18}\text{O}$; (c) precipitation, and (d) deuterium excess. The red line marks $p = 0.05$ statistical significance.

3.3. WA Analysis

The temperature shows a typical graph of seasonal fluctuation within a period of 12 months (Figure 3a), localized at the (12 ± 1) month period. $\delta^{18}\text{O}$ (Figure 3b) and $\delta^2\text{H}$ (Figure S2) graphs also show typical seasonal graphs with slightly lower localization in a 12-month period. Here, we should mention that $\delta^2\text{H}$ and $\delta^{18}\text{O}$ graphs were obtained for 1980–2006 and separately for 2012–2021 because of a large gap in data from 2007 to 2011. However, the same dominant period is observed in both cases.

The WA graph for precipitation and deuterium excess (Figure 3c,d) showed an average period of 12 months, but with much larger fluctuations compared to $\delta^2\text{H}$ and $\delta^{18}\text{O}$ —they contained more non-dominant periods. The deuterium excess graph is also divided into 1980–2006 and 2012–2021 periods with the same characteristics.

WA analysis confirms that the dominant 12-month periodicity is stationary in time.

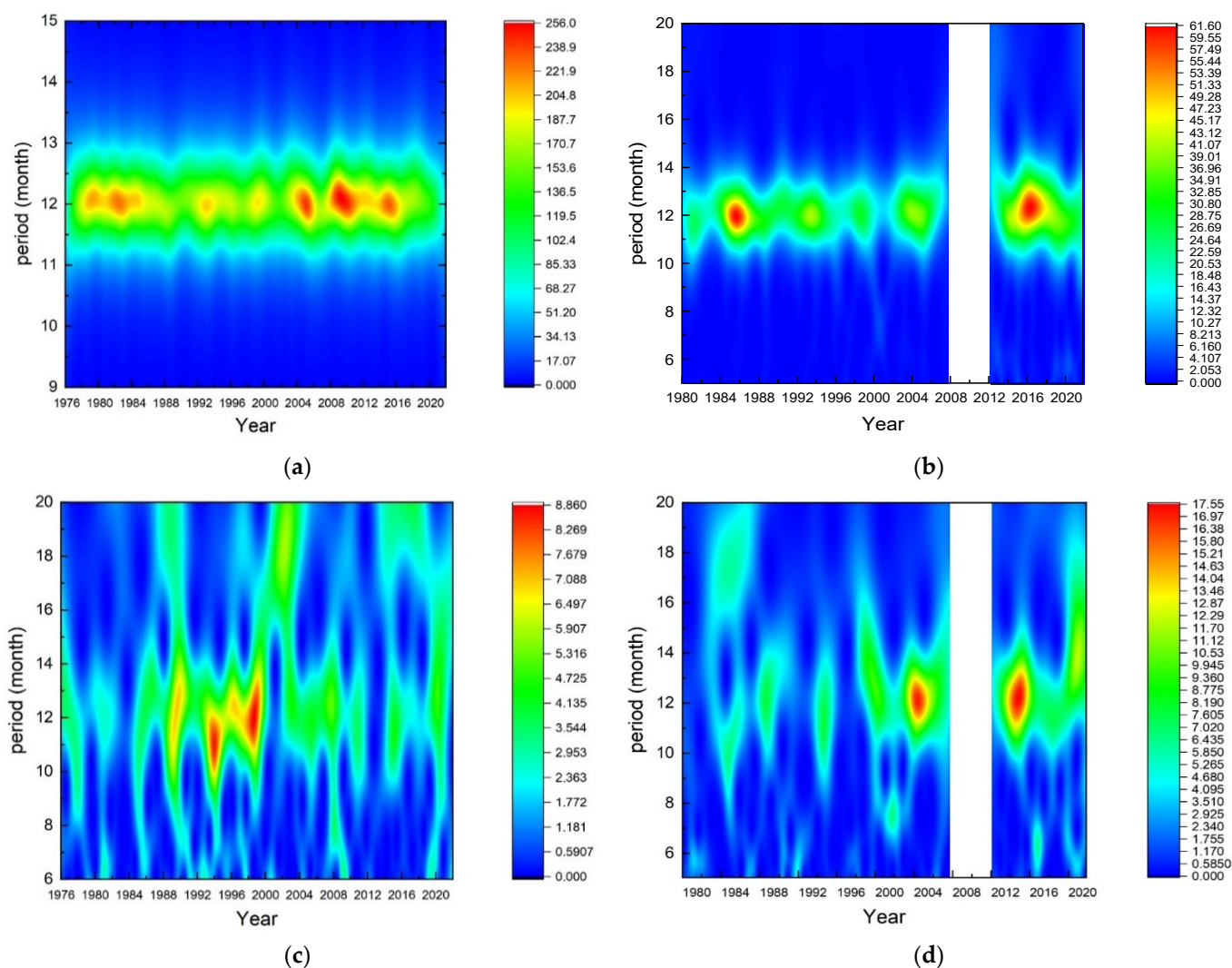


Figure 3. Wavelet analysis (WA) of the: (a) temperature; (b) $\delta^{18}\text{O}$; (c) precipitation amount, and (d) deuterium excess.

3.4. Correlations

Correlations among the studied quantities were quantified by both Pearson’s (r) and Spearman’s (ρ) correlation coefficients for linear and monotonic correlation, respectively (Table 1 and Figure 4). Both gave similar results, and the strongest correlations were found between $\delta^2\text{H}$ and $\delta^{18}\text{O}$ (both r and ρ values > 0.98), temperature and $\delta^2\text{H}$ (both r and ρ values > 0.79), and temperature and $\delta^{18}\text{O}$ (> 0.79), justifying the linear and monotonic correlations. The other quantities showed much weaker or no correlation at all.

Table 1. Pearson’s r and Spearman’s ρ correlation coefficients.

	ρ	$\delta^{18}\text{O}$	$\delta^2\text{H}$	Precipitation	Temperature	Deuterium
	r	(‰)	(‰)	(mm)	(°C)	Excess (‰)
$\delta^{18}\text{O}$ (‰)		-	0.986	0.084	0.799	-0.238
$\delta^2\text{H}$ (‰)		0.988	-	0.117	0.799	-0.098
Precipitation (mm)		0.089	0.127	-	0.246	0.225
Temperature (°C)		0.793	0.799	0.235	-	-0.137
Deuterium excess (‰)		-0.277	-0.126	0.235	-0.155	-

Numbers in bold—significant correlation.

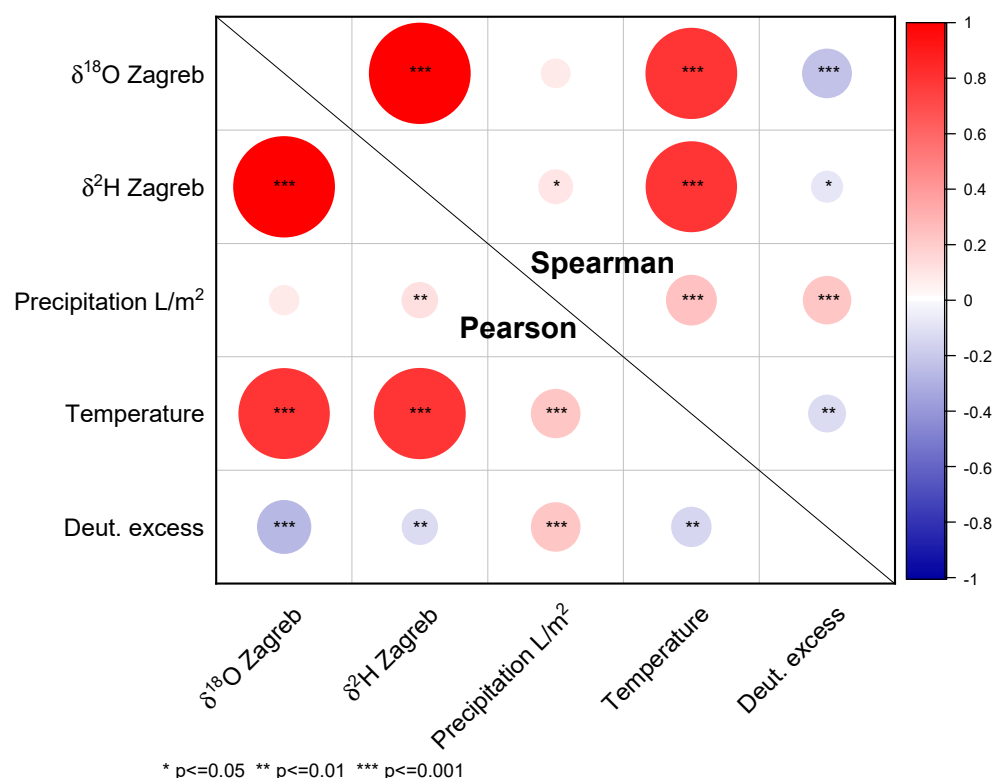


Figure 4. Pearson's r and Spearman's ρ correlation. The correlation strength is shown both in the color and size of the circles. Asterix denotes the statistical significance of the correlation.

4. Conclusions

The time series analyses justified previously observed behavior of temperature, precipitation amount, and stable isotope data in precipitation concerning seasonal periodicity. All used statistical methods indicate a similar behavior pattern of temperature, $\delta^{18}\text{O}$, and $\delta^2\text{H}$. Both FA and WA gave the highest power periodicity for the temperature, followed by $\delta^{18}\text{O}$ and $\delta^2\text{H}$, and finally, the precipitation amount and deuterium excess. FA showed a peak at 12 months, which was confirmed by WA, suggesting a stationary periodicity in time.

However, this kind of analysis does not give information on the long-term temporal change of the parameters, such as the dependence on temperature. This could be an important parameter for relating the stable isotope data in precipitation with the current climate change.

Thus, the results of the current paper present complementary results to the previously published ones. In the future, any analysis of precipitation data for at least 7 years of isotope data will not be considered complete without the following: principal component analysis, Fourier or wavelet analyses, $\delta^{18}\text{O}$ vs. $\delta^2\text{H}$ relation, and $\delta^{18}\text{O}$ vs. temperature or precipitation amount.

Supplementary Materials: The following are available online at <https://www.mdpi.com/article/10.3390/w14132008/s1>, Figure S1: Fourier analysis of $\delta^2\text{H}$; Figure S2: Wavelet analysis of $\delta^2\text{H}$; Table S1: Precipitation amount, temperature, $\delta^{18}\text{O}$, $\delta^2\text{H}$, deuterium excess, and tritium activity concentration in monthly precipitation in Zagreb, 2019–2021.

Author Contributions: Conceptualization, D.B. and I.K.B.; methodology, D.B.; validation, Z.K.; formal analysis, D.B. and I.K.B.; data curation, Z.K.; writing—original draft preparation, D.B. and I.K.B.; writing—review and editing, D.B., Z.K. and I.K.B.; visualization, D.B.; supervision, I.K.B. All authors have read and agreed to the published version of the manuscript.

Funding: This research received no external funding.

Institutional Review Board Statement: Not applicable.

Informed Consent Statement: Not applicable.

Data Availability Statement: Data for 1976–2018 can be found in [14].

Acknowledgments: We thank IAEA project CRO7001 “Isotope Investigation of the Groundwater–Surface Water Interactions at the Well-Field Kosnica in the Area of the City of Zagreb”, 2016–2017, for providing us with the LWIA-45-EP Liquid Water Isotope Analyzer.

Conflicts of Interest: The authors declare no conflict of interest.

References

1. Weedon, G. *Time Series Analysis and Cyclostratigraphy: Examining Stratigraphic Records of Environmental Cycles*; Cambridge University Press: Cambridge, UK, 2008; pp. 1–276.
2. Liu, H.-S.; Chao, B.F. Wavelet spectral analysis of the Earth’s orbital variations and paleoclimatic cycles. *J. Atmos. Sci.* **1998**, *55*, 227. [CrossRef]
3. Debret, M.; Sebagn, D.; Crosta, X.; Massei, N.; Petit, J.-R.; Chapron, E.; Bout-Roumazelles, V. Evidence from wavelet analysis for a mid-Holocene transition in global climate forcing. *Quat. Sci. Rev.* **2009**, *28*, 2675–2688. [CrossRef]
4. Rimbu, N.; Lohman, G.; Werner, M.; Ionita, M. Links between central Greenland stable isotopes, blocking and extreme climate variability over Europe at decadal to multidecadal time scales. *Clim. Dyn.* **2017**, *49*, 649–663. [CrossRef]
5. Sharma, S.; Nalley, D.; Subedi, N. Characterization of Temporal and Spatial Variability of Phosphorus Loading to Lake Erie from the Western Basin Using Wavelet Transform Methods. *Hydrology* **2018**, *5*, 50. [CrossRef]
6. Tognarelli, A.; Zancheta, G.; Regattieri, E.; Isola, I.; Drysdale, R.N.; Bini, M.; Hellstrom, J.C. Wavelet analysis of $\delta^{18}\text{O}$ and $\delta^{13}\text{C}$ time-series from an Holocene speleothem record from Corchia Cave (central Italy): Insights for the recurrence of dry-wet periods in the Central Mediterranean. *Ital. J. Geosci.* **2018**, *137*, 128–137. [CrossRef]
7. Maruyama, F. Relationship between the atmospheric CO_2 and climate indices by wavelet-based multifractal analysis. *J. Geosci. Environ. Prot.* **2019**, *7*, 38.
8. Rezaei, A.; Saatsaz, M. Large-scale climate indices teleconnections with hydrochemical and isotopic characteristics of a karst spring using wavelet analysis. *Environ. Earth Sci.* **2021**, *80*, 335. [CrossRef]
9. Zamrane, Z.; Mahé, G.; Laftouhi, N.-E. Wavelet Analysis of Rainfall and Runoff Multidecadal Time Series on Large River Basins in Western North Africa. *Water* **2021**, *13*, 3243. [CrossRef]
10. Palcsu, L.; Morgenstern, U.; Sültenfuss, J.; Koltai, G.; Laszlo, E.; Temovski, M.; Major, Z.; Nagy, J.T.; Papp, L.; Varlam, C.; et al. Modulation of cosmogenic tritium in meteoric precipitation by the 11-year cycle of solar magnetic field activity. *Sci. Rep.* **2018**, *8*, 12813. [CrossRef] [PubMed]
11. Borković, D.; Krajcar Bronić, I. Solar activity cycles recorded in long-term data on tritium activity concentration in precipitation at Zagreb, Croatia. *Rad. Phys. Chem.* **2021**, *108*, 109646. [CrossRef]
12. Varlam, C.; Dului, O.G.; Ionete, R.E.; Costrinel, D. Time series analysis of the $\delta^2\text{H}$, $\delta^{18}\text{O}$ and d-excess values in correlation with monthly temperature, relative humidity and precipitation in Ramnicu Valcea, Romania: 2012 to 2018. *Geol. Soc. Lond. Spec. Publ.* **2021**, *507*, 77–89. [CrossRef]
13. IAEA/WMO. Global Network of Isotopes in Precipitation. The GNIP Database. Available online: <https://nucleus.iaea.org/wiser> (accessed on 15 May 2021).
14. Krajcar Bronić, I.; Barešić, J.; Borković, D.; Sironić, A.; Lovrenčić Mikelić, I.; Vreća, P. Long-Term Isotope Records of Precipitation in Zagreb, Croatia. *Water* **2020**, *12*, 226. [CrossRef]
15. Horne, J.H.; Baliunas, S.L. A Prescription for Period Analysis of Unevenly Sampled Time-Series. *Astrophys. J.* **1986**, *302*, 757–763. [CrossRef]
16. Press, W.H.; Teukolsky, S.A.; Vetterling, W.T.; Flannery, B.P. *Numerical Recipes in C: The Art of Scientific Computing*, 2nd ed.; Cambridge University Press: Cambridge, UK, 1992; pp. 575–584.
17. Foster, G. Wavelets for period analysis of unevenly sampled time series. *Astron. J.* **1996**, *112*, 1709–1729. [CrossRef]
18. Davis, J.C. *Statistics and Data Analysis in Geology*; John Wiley & Sons: New York, NY, USA, 1986; Volume 646, pp. 548–551.
19. Coplen, T.B.; Wassenaar, L.I. LIMS for Lasers for achieving long-term accuracy and precision of $\delta^2\text{H}$, $\delta^{17}\text{O}$, and $\delta^{18}\text{O}$ of waters using laser absorption spectrometry. *Rapid Commun. Mass Spectrom.* **2015**, *29*, 2122–2130. [CrossRef] [PubMed]